

Photocatalytic reactivity of the titanium oxide loaded on a stainless steel screen by a spraying method

F. Shiraishi,^a T. Itoh,^a Y. Oda,^a H. Nagayoshi,^b T. Higuchi,^b K. Tateishi^c

^a*Department of Systems Design, Bio-Architecture Center, Kyushu University, Fukuoka 812-8581, Japan*

^b*FUJICO Co., Ltd., 4-31, Makiyamashinmachi, Kitakyushu 804-0054, Japan*

^c*I-Quark Corporation, 1-36-14, Matsushima, Higashi-ku, Fukuoka 812-0062, Japan*

Abstract

To reduce a film-diffusional resistance in the very vicinity of the photocatalyst surface, titanium oxide particles containing a small amount of adsorbent particles (3-10 %) are immobilized on a stainless steel screen by a spraying method and its performance is investigated by decomposing 2,4-dinitrophenol in water. It is found that the activity of this photocatalyst screen is higher than that of the photocatalyst glass tube prepared by the conventional dip-coating method in the region of low linear velocity. A simple mathematical model that takes into consideration the photocatalytic reaction, diffusion, and adsorption is used to interpret the experimental result.

Keywords: photocatalyst, spraying method, water purification, film-diffusional resistance, adsorbent particles

1. Introduction

As a result of intensive investigation on the air purification process by an immobilized photocatalyst, the authors previously found that the film-diffusional resistance is the main negative factor that significantly reduces the performance of the photocatalytic decomposition of organic compounds (Xu and Shiraishi, 1999; Shiraishi et al., 2004; Shiraishi et al., 2005a; Shiraishi et al., 2005b) and then developed an air cleaner that succeeded in gaining a high decomposition performance by removing such a diffusional resistance (Shiraishi, 2004; Shiraishi et al., 2004; Shiraishi et al., 2005a; Shiraishi et al., 2005b; Shiraishi et al., 2007). On the other hand, despite huge efforts all over the world, there is no remarkable progress in the application of the photocatalytic water treatment. Of course, if several weeks or months are given for the treatment, the photocatalytic water treatment process by solar irradiation could readily be put to practical use. In actual situation, however, the

treatment should be finished within several hours to days. Why is the practical use of the photocatalytic treatment process difficult in water compared to in air? This is due to a marked decrease in the photocatalytic activity in the water environment (Shiraishi et al., 1999; Wang and Shiraishi, 2002; Wang et al., 2002b, 2002a). That is, in the water environment, the film-diffusional resistance is even more increased, the UV light intensity is markedly reduced, radicals are quickly consumed by water molecules, and the photocatalytic reaction is strongly inhibited by various kinds of coexisting ions.

Although the photocatalytic reactivity may be enhanced by doping metals on titanium oxide (Kanno et al., 1985; Sobczynski et al., 1987; Moon et al., 1998; Jin and Shiraishi, 2003), the presence of other metal(s) may easily cause destabilization of the photocatalytic activity. Moreover, since the photocatalyst is mostly applied to the decomposition of the organic compounds that are usually present at very low concentrations, the presence of the film-diffusional resistance is very serious. In the case of air purification, this problem was easily solved by introducing contaminated air into an annulus at a high linear velocity by an electric fan. Likewise, in the water treatment, supply of the reaction mixture at a very high linear velocity makes it possible to reduce the film-diffusional resistance (Wang and Shiraishi, 2002; Wang et al., 2002a). In a liquid system, however, this method is not economical because an expensive and high-performance water pump is necessary to secure a high circulation linear velocity and a large amount of electrical energy is consumed. Moreover, even if it is possible to flow a liquid solution at a high linear velocity, a shearing stress imposed by water gradually exfoliates the thin photocatalyst film on a support.

The purpose of the present work is to investigate a photocatalytic water treatment system that has a potential to solve the above-mentioned problems. Firstly, to prevent the photocatalyst film from exfoliating in the water treatment at a high linear velocity, we form a strongly adhesive thin film of titanium oxide on a stainless steel screen by a coating technique called a spraying method and then investigate the performance of the prepared photocatalyst screen in the batch recirculation treatment of an aqueous solution containing organic compounds. Secondly, to obtain a satisfactorily high photocatalytic activity at a low linear velocity, we prepare the photocatalyst screen in which adsorbent particles such as zeolite or other adsorbent particles are uniformly distributed and then investigate their decomposition activities. Thirdly, we attempt to interpret characteristics of the experimental data by use of a mathematical model that takes into consideration the photocatalytic reaction, adsorption, and diffusion.

2. Theory

A mathematical model that takes into consideration the facts that the photocatalytic reactions obey a Langmuir-Hinshelwood mechanism (Matthews, 1988; Wang et al., 2002b) and are strongly affected by a film-diffusional resistance is described by (Shiraishi et al., 1996)

$$v = E_r \frac{\alpha k K_H C}{1 + K_H C} \quad (1)$$

Photocatalytic reactivity of the titanium oxide loaded on a stainless steel screen by a spraying method

where v is the rate of the photocatalytic reaction per unit volume of liquid [$\text{g m}^{-3}\text{-liq min}^{-1}$], E_f is the catalytic effectiveness factor [–], k is the rate constant [$\text{g m}^{-2}\text{-cat min}^{-1}$], K_H is the adsorption equilibrium constant [$\text{m}^3 \text{g}^{-1}$], and C is the reactant concentration [g m^{-3}]. Also, α is the specific surface area [$\text{m}^2\text{-cat m}^{-3}\text{-liq}$], given by

$$a_v = S/V_L \quad (2)$$

where S is the apparent surface area of the photocatalyst screen and V_L is the liquid volume. It is a common means to express v in terms of

$$v' = v/a_v \quad (3)$$

where v' is the rate of the photocatalytic decomposition per unit apparent surface area of the photocatalyst screen [$\text{g m}^{-2}\text{-cat min}^{-1}$].

In the absence of negligible film-diffusional resistance, initial rates of photocatalytic decomposition v_0 are measured at various initial reactant concentrations C_0 by use of the photocatalyst screen. These values are then converted into v'_0 according to Eq. (3). Since $E_f=1$, the linearized form of Eq.(1) is given by

$$\frac{C_0}{v'_0} = \frac{1}{k}C_0 + \frac{1}{k K_H} \quad (4)$$

Therefore, Eq.(4) is applied to the experimental data in order to obtain the values of the slope and intercept of the straight line by the least-square method. These values are then used to determine the values of k and K_H .

The actual photocatalytic reaction occurs in the presence of film-diffusional resistance. The effectiveness factor that includes this effect is given by

$$E_f = \frac{(1 + \beta_b)\{\beta_b + \phi + 1 - \sqrt{(\phi + 1 - \beta_b)^2 + 4\beta_b}\}}{2\beta_b\phi} \quad (5)$$

where

$$\beta_b = C_0 K_H \quad (6)$$

$$\phi = k K_H / k_L \quad (7)$$

in which β_b is the dimensionless reactant concentration, ϕ is the modulus, and k_L is the mass-transfer coefficient. The value of k_L changes with the magnitude of the linear velocity and is generally expressed in terms of the following expression (Lortie and Thomas, 1986; Shiraishi et al., 1996; Miyakawa and Shiraishi, 1997).

$$k_L = a u^b \quad (8)$$

It is now easy to estimate that the film-diffusional resistance changing with the linear velocity has an effect on the rate of the photocatalytic decomposition. To include this effect into the mathematical model, the constants a and b in Eq. (8) must be determined. For this purpose, we apply the algebraic equation:

$$f(k_L) = v_0^{\text{exp}} - v_0^{\text{calc}} \quad (9)$$

to the experimental values obtained by use of the photocatalyst screen without adsorbent particles and fit the calculated values v_0^{calc} to the corresponding experimental values v_0^{exp} by the Newton-Raphson method so that the value of k_L can be determined for each linear velocity u . The details of the root-finding procedure

used are described elsewhere (Shiraishi et al., 2006). A least-square method is applied to a plot of $\log k_L$ against $\log u$ to determine a and b in Eq. (8). As a result, the expression for k_L is determined as a function of u .

To interpret characteristics of the experimental data obtained by use of the photocatalyst screen containing zeolite particles, we include the term expressing the adsorption of reactant molecules onto zeolite particles into the mathematical model. For simplicity, we introduce the effectiveness given by

$$E_f = \frac{(1 + \beta_b) \{ \beta_b + \phi + e^\lambda - \sqrt{(\phi + e^\lambda - \beta_b)^2 + 4e^\lambda \beta_b} \}}{2\beta_b \phi} \quad (10)$$

where the adsorption factor λ takes a negative value and its absolute value becomes larger as the reactant concentration on the photocatalyst surface increases owing to an action of adsorbent particles. Although Eq. (10) is originally the effectiveness factor used in an immobilized enzyme reaction system (Shuler et al., 1972; Shiraishi, 1997) where an electrostatic interaction is present between the reactant molecule and enzyme support, we simply replace the effect of electrostatic attraction by the effect of adsorption. Thus, Eq. (1) with Eq. (10) is applied to the experimental data obtained by use of the photocatalyst screen containing zeolite particles and the calculated values are fit to the experimental ones so that the value of λ can be determined.

3. Experimental method

The reactant was 2,4-dinitrophenol (DNP) and the photocatalyst was titanium oxide fine particles in anatase form (Wako Pure Chemical Industries, Ltd., Osaka, Japan). Three kinds of adsorbent particles were tested; zeolite with pore sizes of 3, 4, and 9 Å (Wako Pure Chemical Industries, Ltd.), activated carbon pellets (Wako Pure Chemical Industries, Ltd.) finely milled with a pestle in a mortar, apatite from cow's leg bone (Bioclean Co., Ltd., Fukuoka, Japan). Titanium oxide particles or those well-mixed with adsorbent particles in order to uniformly distribute them in a titanium oxide particle layer were sprayed onto a stainless steel screen where the wire diameter and the gap between wires are both 0.1 mm. The contents of zeolite particles distributing in a titanium oxide particle layer were 3, 5, and 10 %.

The photocatalyst screen thus prepared was cut in a size of 14 cm × 8.8 cm and mounted in the annular-flow reactor shown in Fig.1 so as to give a close contact with its inside wall. This reactor has a 6W blacklight blue fluorescent lamp (FL6BLB; Toshiba Co., Ltd., Tokyo, Japan) and a quartz glass tube for its protection. The details of the reactor structure are described elsewhere (Shiraishi et al., 2003; Shiraishi and Kawanishi, 2004). A reaction mixture that entered the reactor was photocatalytically treated when flowing through an annulus between the photocatalyst screen and the outer surface of the quartz glass tube (about 5 mm in annular gap).

The photocatalytic reactor was connected to a perfectly-mixed container and a peristaltic pump (RP 1000; Eyela, Tokyo, Japan), and then operated in batch recirculation mode (Shiraishi et al., 2006). In every experiment, we treated 5.0×10^{-4} m³ of an aqueous DNP solution to determine the initial rate of the DNP

Photocatalytic reactivity of the titanium oxide loaded on a stainless steel screen by a spraying method

decomposition by measurement of an absorbance at 357 nm with a spectrophotometer (UV mini 1240; Shimadzu, Kyoto, Japan).

4. Results and discussion

4.1 Effect of zeolite pore size on the initial rate of DNP decomposition

To measure the initial rates of DNP decomposition, we treated 10 g m^{-3} aqueous DNP solutions flowing at low linear velocities of $0.0298\text{--}0.0115\text{ m s}^{-1}$ by use of the photocatalyst screens containing 5 % of zeolite particles with pore sizes of 3, 4, and 9 Å. The result is shown in Fig. 2. The initial rates of DNP decomposition for different pore sizes of zeolite have no remarkable difference at any linear velocity. Therefore, we simply used 4 Å zeolite particles in the following experiment, although the optimal pore size may be related to the size of a reactant molecule,.

4.2 Effect of zeolite content on the initial rate of DNP decomposition

To measure the initial rates of DNP decomposition, we treated 10 g m^{-3} aqueous DNP solutions flowing at a linear velocity of 0.006 m s^{-1} by use of the photocatalyst screens containing 3-10 % of zeolite particles with a pore size of 4 Å. The result is shown in Fig. 3. The initial rate of DNP decomposition increases as the zeolite content increases up to 5 %. This is considered due to an increase in the DNP concentration in the vicinity of photocatalyst surface as a result of adsorption of DNP molecules onto zeolite particles. However, the initial rate decreases when the zeolite content further increases up to 10 %. This is considered due to a decrease in the amount of titanium oxide exposed at the surface of the photocatalyst screen. The result indicates that the 5% zeolite content is optimum in this photocatalytic reaction system. In the following experiment, therefore, we used the photocatalyst screen with a zeolite content of 5 %.

4.3 Effect of kind of adsorbent particles on the initial rate of DNP decomposition

To measure the initial rates of DNP decomposition, we treated 10 g m^{-3} aqueous DNP solutions flowing at low linear velocities of $0.0298\text{--}0.0512\text{ m s}^{-1}$ by use of the photocatalyst screens containing zeolite particles of 4 Å, activated carbon particles, or apatite particles. The contents of these adsorbents were all 5 %. The result is shown in Fig. 4. The initial rate of DNP decomposition for the zeolite particles increases with the increase of the linear velocity. A comparison of the decomposition rate for zeolite with the decomposition rates for other adsorbents in the region of low linear velocity clearly shows that the photocatalyst screen containing zeolite particles has the largest activity. Although we had an estimation that the activity of the photocatalyst screen containing activated carbon particles would be much higher than others, it is clear that the activity is not high. This is probably due to a significant drop in the ability of activated carbon particles to adsorb DNP molecules because when the spray coating was carried out, the surface temperature of the titanium oxide film was instantaneously increased to about $700\text{ }^{\circ}\text{C}$ so that activated carbon particles were oxidized. Therefore, a spraying method in nitrogen atmosphere should be investigated in the future. On the other hand, the photocatalyst screen containing apatite has a very

low activity. This is probably due to its low adsorption ability compared with others and also inhibition of the photocatalytic reaction as a result of elution of apatite to the solution.

4.4 Effect of linear velocity of a reaction mixture on the initial rate of DNP decomposition

Figure 5 shows the relationship between the initial rate of DNP decomposition and the linear velocity of a reaction mixture in the annular-flow reactor. In the region of low linear velocity, the initial rate of DNP decomposition for the photocatalyst screen prepared by the spraying method is larger than that for the photocatalyst glass tube prepared by the conventional dip-coating method (Shiraishi et al., 2003; Shiraishi and Kawanishi, 2004). In addition, when zeolite particles are contained, the initial rate of DNP decomposition is further increased. For example, at a linear velocity of 0.005 m s^{-1} , the photocatalytic activity of the photocatalyst screen is higher by about two times than that of the dip-coating method. This is considered due to a reduction in the film-diffusional resistance in the region of low linear velocity as a result of the attraction of DNP molecules toward the photocatalyst surface by zeolite particles. The low linear velocity region is practical in the meaning that a fewer amount of electrical energy is consumed and photocatalyst film is not easily exfoliated because the solution is allowed to flow moderately.

4.5 SEM observation of a titanium oxide film immobilized by the spraying method

In the present work, we found that the photocatalytic activities of titanium oxide particles and those containing zeolite particles are superior to that of the titanium oxide particles prepared by the dip-coating method in the region of low linear velocity. To interpret this result, we observed the titanium oxide film on the screen surface. The result is shown in **Fig.6**. It is obvious that the titanium oxide film prepared by the spraying method is composed of a lump of large titanium oxide particles and has an uneven surface. As a result, we estimate that the photocatalyst screen has a larger specific surface area and gives a higher rate of the DNP decomposition. It can be predicted from the principle of the spraying method that zeolite particles are uniformly distributed in the titanium oxide particle layer. Although we tried to confirm it from the SEM photographs, it was difficult to distinguish zeolite particles from titanium oxide particles.

4.6 Interpretation of experimental data using a photocatalytic reaction model

One of the advantages of the spraying method is that it is possible to form a uniform distribution of adsorbent particles in the photocatalyst film. In such an environment, it is expected that the reactant is first adsorbed on zeolite particles and then decomposed by titanium oxide particles, thereby increasing the rate of photocatalytic decomposition. To confirm the validity of this estimation, we attempted to interpret the experimental result by use of a mathematical model that takes into consideration the diffusion of a reactant through the film in the very vicinity of photocatalyst surface, the adsorption of the reactant onto zeolite particles uniformly distributed in the titanium oxide film, and the photocatalytic decomposition of the reactant adsorbed.

The apparent surface area of the photocatalyst screen S has a value of $1.23 \times 10^{-2} \text{ m}^2\text{-cat}$ and the liquid volume V_L has a value of $5.0 \times 10^{-4} \text{ m}^3\text{-liq}$. Therefore, the specific surface area α takes a value of $24.6 \text{ m}^2\text{-cat m}^{-3}\text{-liq}$. Firstly, DNP was decomposed at various initial concentrations by use of the photocatalyst screen without adsorbent particles to measure the initial rates of DNP decomposition per unit volume of liquid v_0 . The measurements were performed at a sufficiently high linear velocity of 0.05 m s^{-1} so that the film-diffusional resistance was negligible. Secondly, the values of v_0 were converted into those of v'_0 according to Eq.(3). **Figure 7** shows a linearized plot of the experimental data in the functional relationship of Eq. (4). The least-square method was applied to the experimental data, which resulted in the following expression.

$$\frac{C_0}{v'_0} = 0.03473C_0 + 0.6813 \quad (11)$$

A comparison of Eq. (11) with Eq. (4) gives $k = 28.8 \text{ g m}^{-2}\text{-cat min}^{-1}$ and $K_H = 0.0510 \text{ m}^3 \text{ g}^{-1}$. On the other hand, an actual photocatalytic reaction takes place in the presence of film-diffusional resistance. Therefore, Eq. (9) was applied to the experimental values obtained by the photocatalyst screen without adsorbent particles in Fig. 5 and the mass-transfer coefficients k_L were determined for individual experimental data by the Newton-Raphson method. **Figure 8** shows the plot of k_L against u . Application of the least-square method to the data plot finally gives the following expression for k_L .

$$k_L = 0.00903 u^{0.236} \quad (12)$$

As shown in Fig. 8, the calculated line using Eq. (12) is in a good agreement with the experimental values, indicating that the mass-transfer coefficient rises in proportion with the linear velocity to the power of 0.236.

Furthermore, Eq. (1) with Eq. (10) was applied to the experimental data obtained by the use of the photocatalyst screen containing zeolite particles and the value of λ was determined by fitting the calculated values to the experimental data. As a result, we obtained $\lambda = -0.75$. As shown in **Fig.9**, the calculated lines for the photocatalyst screen with and without zeolite particles satisfactorily express the variations in the corresponding experimental data, which suggests that the DNP decomposition by the photocatalyst screen containing zeolite particles was improved by the adsorption of DNP onto zeolite particles.

5. Conclusions

The photocatalytic water treatment produces the following two serious problems; the significant decrease in the rate of photocatalytic decomposition by the film-diffusional resistance and the separation of the photocatalyst film by the shearing stress imposed by water flowing at a high linear velocity. To solve these problems, a strongly adhesive thin film of titanium oxide particles was formed on a stainless steel screen by the spraying method and DNP was then photocatalytically decomposed. As a result, the following conclusions were drawn.

- 1) The rate of the photocatalytic decomposition of DNP for the photocatalyst screen prepared by the spraying method was higher than that for the photocatalyst glass tube prepared by the conventional dip-coating method. The activity of the photocatalyst screen containing zeolite particles was even more enhanced. This is considered due to an increase in the DNP concentration in the vicinity of photocatalyst surface as a result of adsorption of DNP on zeolite particles.
- 2) There is no marked effect of zeolite pore sizes on the rate of the photocatalytic decomposition as far as the DNP decomposition is concerned.
- 3) The maximum activity of the photocatalyst screen containing zeolite particles appears at a 5 % zeolite content.
- 4) An increase in the rate of DNP decomposition by addition of zeolite particles can successfully be explained by a mathematical model that takes into consideration the diffusion of DNP molecules through the film in the very vicinity of photocatalyst surface, the adsorption of DNP on zeolite particles, and the subsequent photocatalytic decomposition of DNP.
- 5) The tough titanium oxide film containing zeolite particles prepared by the spraying method is useful for the water treatment because it can reduce the film-diffusional resistance and then decompose organic compounds at a higher rate.

Acknowledgment

This work was supported by Grant-in Aid for Scientific Research (C) (18560733), The Ministry of Education, Culture, Sports, Science and Technology.

References

- Jin, S., Shiraishi, F., (2003) Enhanced photocatalytic decompositions of organic compounds over metal-photodepositing titanium dioxide, *Chem. Eng. J.*, 97, 203-211.
- Kanno, H., Yamamoto, Y., Harada, H., (1985) TiO₂-based photocatalysts prepared from titanium isopropoxide and aqueous electrolyte solutions, *Chem. Phys. Lett.*, 121, 245-248.
- Lortie, R., Thomas, D., (1986) Heterogeneous one-dimensional model for fixed bed enzyme reactors, *Biotechnol. Bioeng.*, 28, 1256-1260.
- Matthews, R. W., (1988) Kinetics of photocatalytic oxidation of organic solutes over titanium dioxide, *J. Catal.*, 111, 264-272.
- Miyakawa, H., Shiraishi, F., (1997) A film diffusional effect on the apparent kinetic parameters in packed-bed immobilized enzyme reactors, *J. Chem. Technol. Biotechnol.*, 69, 456-462.

Photocatalytic reactivity of the titanium oxide loaded on a stainless steel screen by a spraying method

Moon, S. C., Mametsuka, H., Suzuki, E., Nakahara, Y., (1998) Characterization of titanium-boron binary oxides and their photocatalytic activity for stoichiometric decomposition of water, *Catalysis Today*, 45, 79084-79084.

Shiraishi, F., *Computational methods for analysis of immobilized enzyme reactions: from reaction kinetics to reactor-design methods*, Corona, Tokyo (1997).

Shiraishi, F., Characteristics of immobilized photocatalytic reaction process and a proposal to its practical use. In: Ampo, S. (Eds.), *Highly-functional photocatalyst: from fundamentals to applications*, NTS, Tokyo, pp. 147-160 (2004).

Shiraishi, F., Ikeda, S., Kamikariya, N., Rapid purification of atmosphere in a closed system. In: *Inter. Symp. on closed habitation experiments material circulation technology*, ed. Tako, Y., Rokkasho, Japan, pp. 426-430 (2004).

Shiraishi, F., Kawanishi, C., (2004) An effect of diffusional film on formation of hydrogen peroxide in photocatalytic reactions, *J. Phys. Chem. A.*, 108, 10491-10496.

Shiraishi, F., Miyakawa, H., Hasegawa, T., Kasai, S., (1996) A computational method for determination of the mass-transfer coefficient in packed-bed immobilized enzyme reactors, *J. Chem. Technol. Biotechnol.*, 66, 405-413.

Shiraishi, F., Nagano, M., Wang, S., (2006) Characterization of a photocatalytic reaction in a continuous-flow recirculation reactor system, *J. Chem. Technol. Biotechnol.*, 81, 1039-1048.

Shiraishi, F., Nakasako, T., Hua, Z., (2003) Formation of hydrogen peroxide in photocatalytic reactions, *J. Phys. Chem. A.* 107, 11072-11081.

Shiraishi, F., Nomura, T., Yamaguchi, S., Ohbuchi, Y., (2007) Rapid removal of trace HCHO from indoor air by an air purifier consisting of a continuous concentrator and photocatalytic reactor and its computer simulation, *Chem. Eng. J.*, 127, 157-165.

Shiraishi, F., Ohkubo, D., Toyoda, K., Yamaguchi, S., (2005a) Decomposition of gaseous formaldehyde in a photocatalytic reactor with a parallel array of light sources: 1. Fundamental experiment for reactor design, *Chem. Eng. J.*, 114, 153-159.

Shiraishi, F., Toyoda, K., Fukinbara, S., Obuchi, E., Nakano, K., (1999) Photolytic and photocatalytic treatment of an aqueous solution containing microbial cells and organic compounds in an annular-flow reactor, *Chem. Eng. Sci.*, 54, 1547-1552.

Shiraishi, F., Toyoda, K., Miyakawa, H., (2005b) Decomposition of gaseous formaldehyde in a photocatalytic reactor with a parallel array of light sources: 2. Reactor performance, *Chem. Eng. J.*, 114, 145-151.

Shuler, M. L., Aris, R., Tsuchiya, H. M., (1972) Diffusive and electrostatic effects with insolubilized enzymes, *J. theor. Biol.*, 35, 67-76.

Sobczynski, A., Bard, A. J., Campion, A., Fox, M. A., Mallouk, T., Webber, S. E., White, J. M., (1987) Photoassisted hydrogen generation: Pt and CdS supported on separate particles, *J. Phys. Chem.*, 91, 3316-3320.

Wang, S., Shiraishi, F., (2002) Decomposition of formic acid in two types of photocatalytic reactors: Effects of film-diffusional resistance and penetration of UV light on decomposition rates, *Eco-Engineering*, 14, 9-17.

Wang, S., Shiraishi, F., Nakano, K., (2002a) Decomposition of formic acid in a photocatalytic reactor with a parallel array of four light sources, *J. Chem. Technol. Biotechnol.*, 77, 805-810.

Wang, S., Shiraishi, F., Nakano, K., (2002b) A synergistic effect of photocatalysis and ozonation on decomposition of formic acid in an aqueous solution, *Chem. Eng. J.*, 87, 261-271.

Xu, J.-H., Shiraishi, F., (1999) Photocatalytic decomposition of acetaldehyde in air over titanium dioxide, *J. Chem. Technol. Biotechnol.*, 74, 1096-1100.

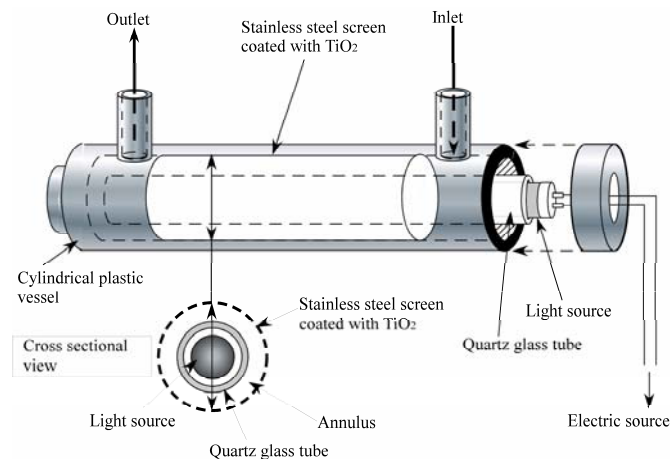


Fig.1 Schematic diagram of an annular-flow photocatalytic reactor

Photocatalytic reactivity of the titanium oxide loaded on a stainless steel screen by a spraying method

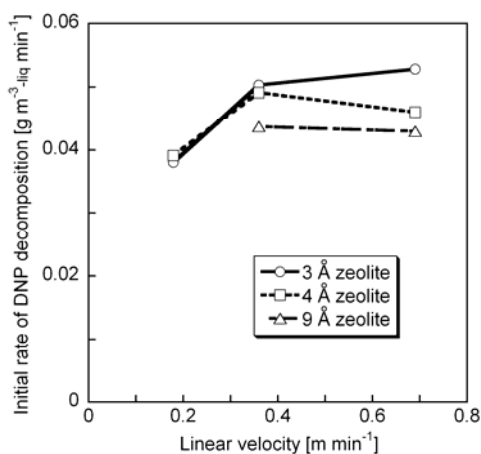


Fig.2 Effect of zeolite pore size on initial rate of DNP decomposition

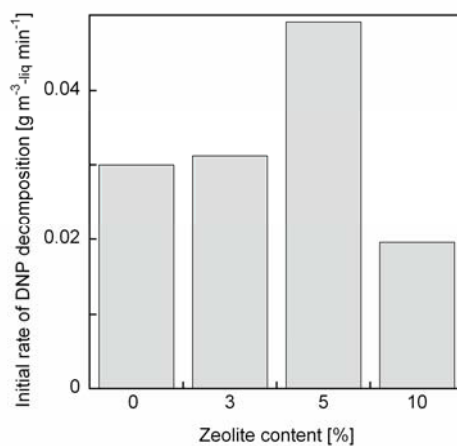


Fig3 Effect of zeolite content on initial rate of DNP decomposition

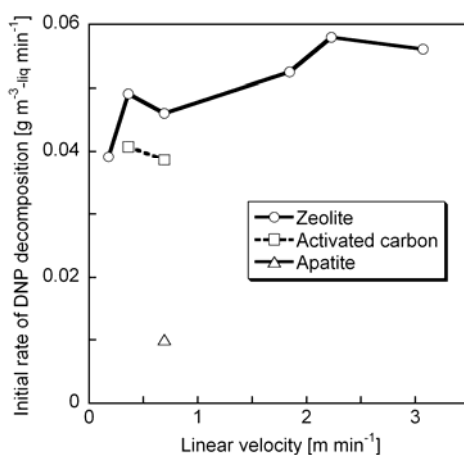


Fig.4 Effect of kind of adsorbents on initial rate of DNP decomposition

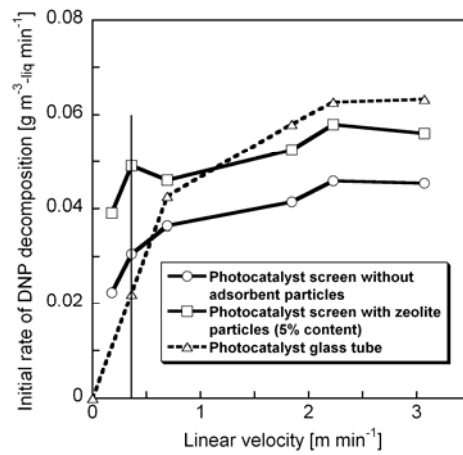


Fig.5 Effect of linear velocity on initial rate of DNP decomposition

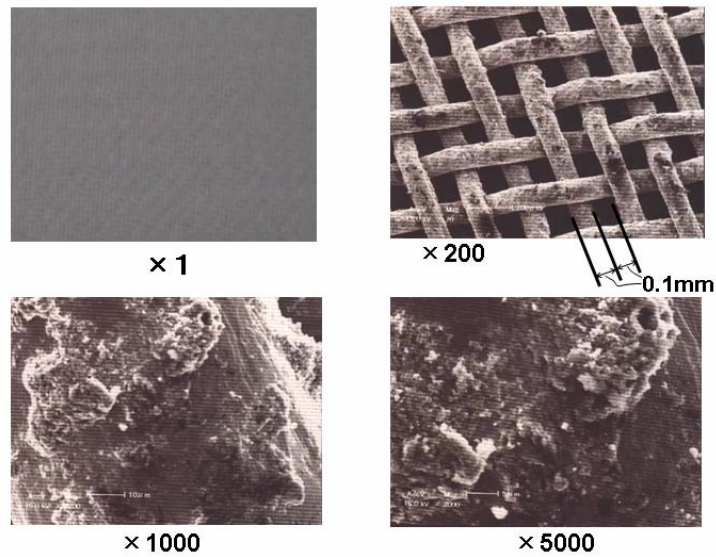


Fig.6 SEM photographs of photocatalyst surface formed on a stainless steel screen by a spraying method

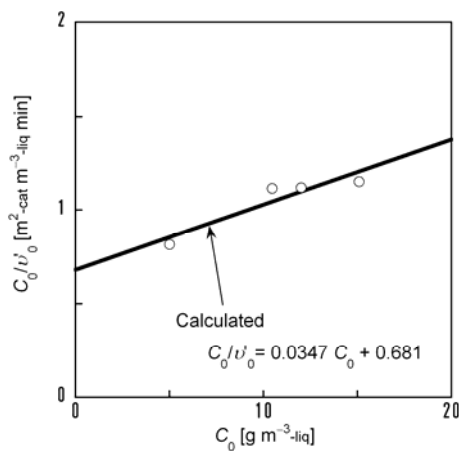


Fig.7 A linearized plot of C_0/v_0 against C_0

Photocatalytic reactivity of the titanium oxide loaded on a stainless steel screen by a spraying method

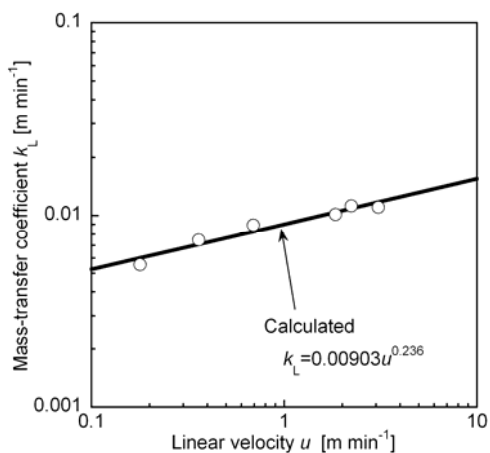


Fig.8 Relationship between mass-transfer coefficient and linear velocity

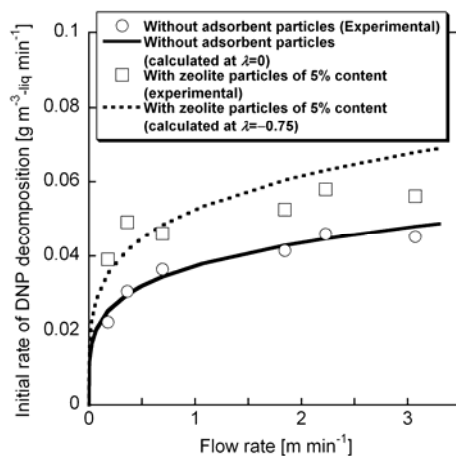


Fig.9 Calculated results for effects of linear velocity on initial rates of DNP decompositions using photocatalyst screens with and without zeolite particles